Journal of Anesthesia (2025) 39:231–247
https://doi.org/10.1007/s00540-024-03451-0

ORIGINAL ARTICLE

Visualization of primary afferent-evoked excitation of spinal dorsal horn neurons using an intracellular Ca^{2+} imaging technique in adult rat spinal cord slices

Hiroshi Baba[1] · **Nobuko Ohashi**[1]

Received: 8 November 2024 / Accepted: 21 December 2024 / Published online: 5 January 2025

Abstract

Purpose Intracellular Ca^{2+} imaging is a valuable tool for studying neuronal activity; however, its application in the spinal cord of mature animals remains underdeveloped. This study aimed to establish an intracellular Ca^{2+} imaging method in adult rat spinal cord slices without complex genetic modifications and characterize primary afferent-evoked intracellular Ca^{2+} responses in spinal dorsal horn neurons.

Methods L5 lumbar spinal cord slices from adult rats were stained with a Ca^{2+} indicator. The relationship between intracellular Ca^{2+} signals and electrophysiological responses induced by dorsal root stimulation was examined. Additionally, the effects of analgesics, anesthetics, and hyperalgesics on the Ca^{2+} responses were analyzed.

Results Monophasic intracellular Ca^{2+} responses were observed with A-fiber intensity stimulation, while biphasic responses were noted with C-fiber intensity stimulation. These responses were not photobleached after repeated measurements (n = 12). The rising phase of Ca^{2+} responses coincided with action potential generation, whereas the falling phase did not. Dorsal root stimulation-induced Ca^{2+} responses were significantly suppressed by morphine (10 μM, 43.9 ± 4.9% of control, n = 8) but not by remimazolam (10 μM, 98.0 ± 2.0% of control, n = 8). Conversely, bicuculline (40 μM, 288.4 ± 48.4% of control, n = 10) and high concentrations of tranexamic acid (3, 10 mM, 132.6 ± 19.9%, 152.6 ± 25.3%, respectively, n = 8) significantly enhanced Ca^{2+} responses.

Conclusion This is a simple and effective approach to examining the effects of drugs that target the spinal cord and investigating nociceptive transmission and modulation mechanisms in the spinal dorsal horn.

Keywords Intracellular Ca^{2+} imaging · Spinal cord slice · Neuronal activity · Dorsal root stimulation · Whole-cell patch-clamp

Introduction

Rapid imaging of intracellular calcium concentrations ($[Ca^{2+}]_{in}$) facilitates spatial and chronological analyses of neuronal activity within the central nervous system [1–4]. Consequently, transgenic mice or rats with genetically encoded Ca^{2+} indicators are increasingly available both technically and commercially [5]. However, their use requires specialized equipment that is not always available in all laboratories. Conversely, staining neural tissues with exogenous Ca^{2+} indicators has been widely used because they do not require complex genetic manipulation. However, in conventional methods for staining mature animal brainstem and spinal cord tissues with exogenous Ca^{2+} indicators, the fluorescence intensity response to afferent input is typically weak; photobleaching from repetitive stimulation and recording is a significant concern [6, 7]. Therefore, studying the subtle effects of drugs and peripheral nerve injury on neuronal activity in these tissues using $[Ca^{2+}]_{in}$ imaging techniques is challenging. One primary challenge is that exogenous dyes difficultly penetrate myelin-rich tissues, such as the medulla oblongata and spinal cord, of mature animals. Achieving adequate Ca^{2+} indicator uptake in the neurons of such tissues can take several hours. However, maintaining the viability of thick spinal cord slices from

✉ Hiroshi Baba
baba@med.niigata-u.ac.jp

[1] Division of Anesthesiology, Niigata University Graduate School of Medical and Dental Science, 1-757 Asahimachi-dori, Chuo-ku, Niigata 951-8510, Japan

mature rats for extended periods requires continuous, rapid perfusion of highly oxygenated artificial cerebrospinal fluid (ACSF) [8, 9].

This study aimed to (1) develop a method for keeping spinal cord slices viable in a staining solution for several hours without continuous perfusion, thereby ensuring adequate uptake of Ca^{2+} indicators by spinal cord neurons, (2) confirm that this improved method yields larger and more stable $[Ca^{2+}]_{in}$ optical responses with reduced photobleaching, and (3) determine the relationship between intracellular Ca^{2+} signals and electrophysiological responses evoked by dorsal root stimulation. Additionally, we aimed to investigate the effects of analgesics, anesthetics, and hyperalgesic drugs on the visualization of neuronal excitation in the spinal dorsal horn.

Materials and methods

Animals and study approval

The study protocol was approved by the Animal Use and Care Committee of Niigata University (Niigata, Japan; approval no. SA00546). Experiments were performed in adult male Wistar rats (10–15 weeks old, 350–450 g). Animal care and use adhered to the guidelines established by the International Association for the Study of Pain. The rats were housed in cages (2–3 rats per cage) under a standard 12-h light–dark cycle with food and water available ad libitum. Room temperature was maintained at 24–26 °C. All efforts were made to minimize animal suffering and reduce the number of animals used.

Adult rat spinal cord slice preparation

The procedure for obtaining adult rat spinal cord slices with an attached dorsal root has been previously described in

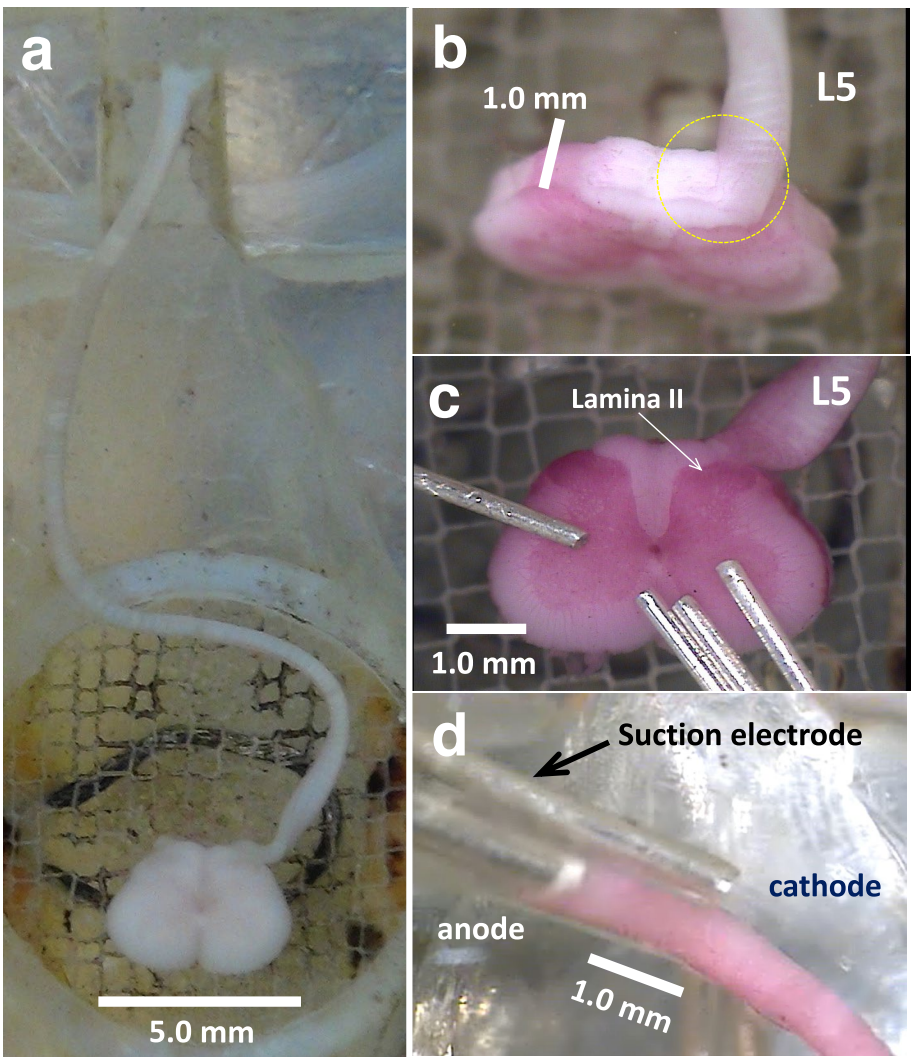

Fig. 1 Preparation of adult rat spinal cord slices for intracellular Ca^{2+} imaging and whole-cell patch-clamp recording. **a** L5 spinal cord slice with a left dorsal root before staining. **b** View from the dorsal side of the spinal cord slice with the attached left L5 dorsal root. The entry zone (surrounded by the yellow dotted circle) is preserved. **c** A spinal cord slice was placed on a nylon mesh after staining with a Ca^{2+} indicator (Rhod-2 AM). Lamina II (substantia gelatinosa; SG) is discernible as a relatively dense band across the superficial dorsal horn. **d** Suction electrode for electrical stimulation of the dorsal root. Depolarizing activity in dorsal horn neurons was evoked by a single-pulse stimulus administered to the L5 dorsal root through a suction electrode

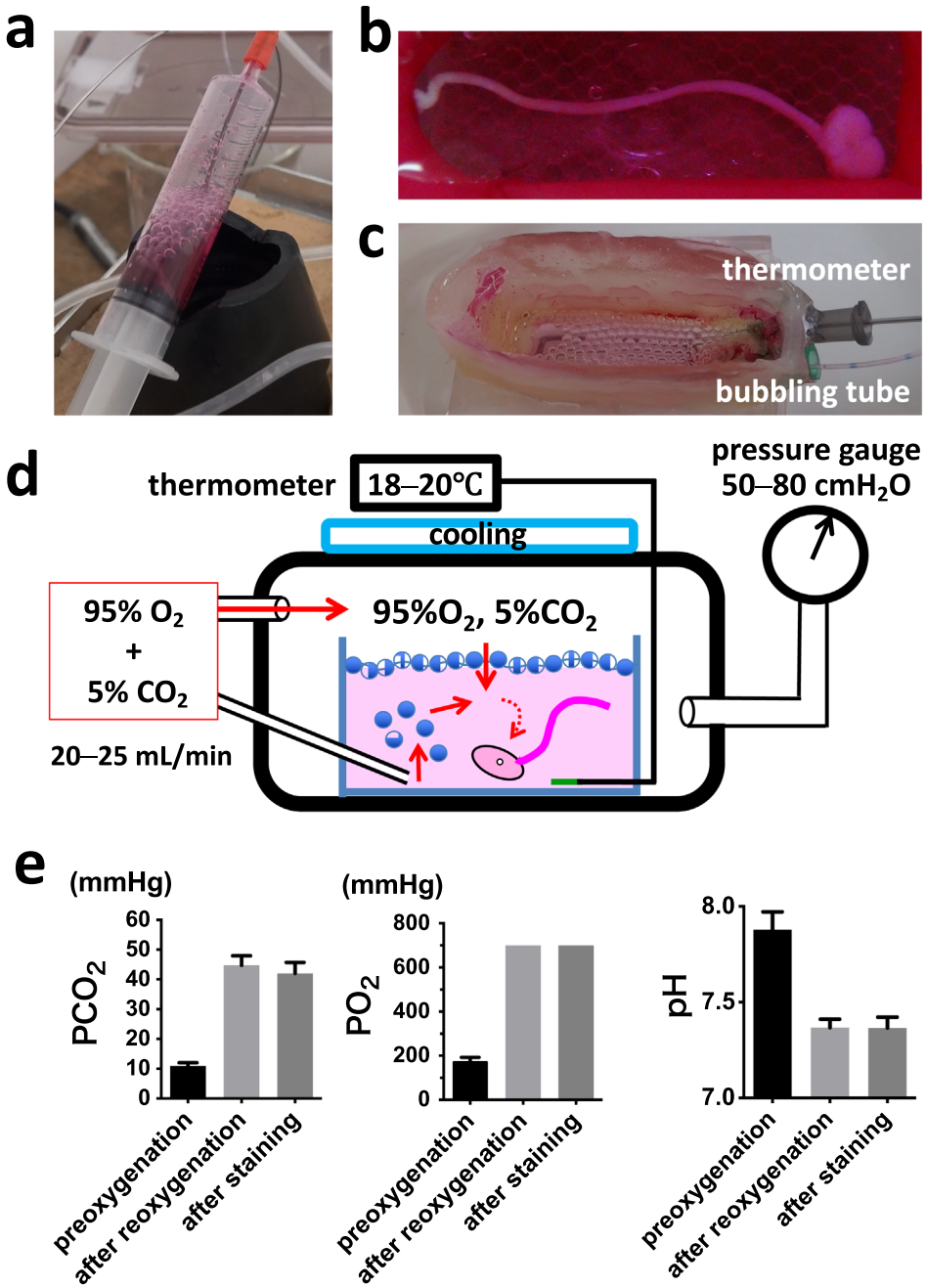

Fig. 2 Methods for staining spinal cord slices using a Ca^{2+} indicator. **a** After Rhod-2 AM (Ca^{2+} indicator) was dissolved in oxygenated ACSF (3.3 mL), the staining solution was further bubbled through a 10-mL syringe with a gas mixture (95% O_2 and 5% CO_2). **b** A spinal cord slice in staining solution. **c** A staining chamber with temperature sensor and bubbling tube. **d** Schematic representation of the oxygen supply during staining. The temperature of the staining solution, the mixed gas flow rate, and the internal pressure in the sealed container were continuously monitored throughout the dyeing process. **e** PCO_2, PO_2, and the pH of the staining solution were maintained at 40–50 mmHg, > 700 mmHg, and approximately 7.4, respectively. Data are presented as mean ± SD (n = 8). The gas analyzer used could not measure oxygen partial pressures above 700 mmHg. *ACSF* artificial cerebrospinal fluid

details [10]. Briefly, a dorsal laminectomy was performed under anesthesia with isoflurane inhalation (1.0–1.5%) and intraperitoneal urethane (1.5 g/kg); a lumbosacral segment of the spinal cord was then extracted. The isolated spinal cord was placed in preoxygenated cold ACSF (2–4 °C). A transverse slice (thickness: 700–750 µm) was cut, preserving the left L5 dorsal root (20–25 mm) (Fig. 1a–d) using a vibrating tissue slicer (Neo LinearSlicer; Dosaka, Kyoto, Japan). Preservation of the long dorsal root was crucial for avoiding direct stimulation of the dorsal horn neurons or entry zone fibers (Fig. 1a, b). The slice was then transferred into a recovery chamber (volume: 0.7 mL) and was superfused with ACSF (15–20 mL/min) equilibrated with a gas mixture of 95% O_2 and 5% CO_2 at room temperature (20–23 °C) for 60 min before staining with a Ca^{2+} indicator. The ACSF composition was as follows (in mM): NaCl: 117, KCl: 3.6, $CaCl_2$: 2.5, $MgCl_2$: 1.2, NaH_2PO_4: 1.2, $NaHCO_3$: 25, and D-glucose: 11. The gas partial pressures of O_2 and CO_2 in the staining solution were measured using a blood gas analyzer (GEM PREMIER 5000, IL Japan, Tokyo, Japan).

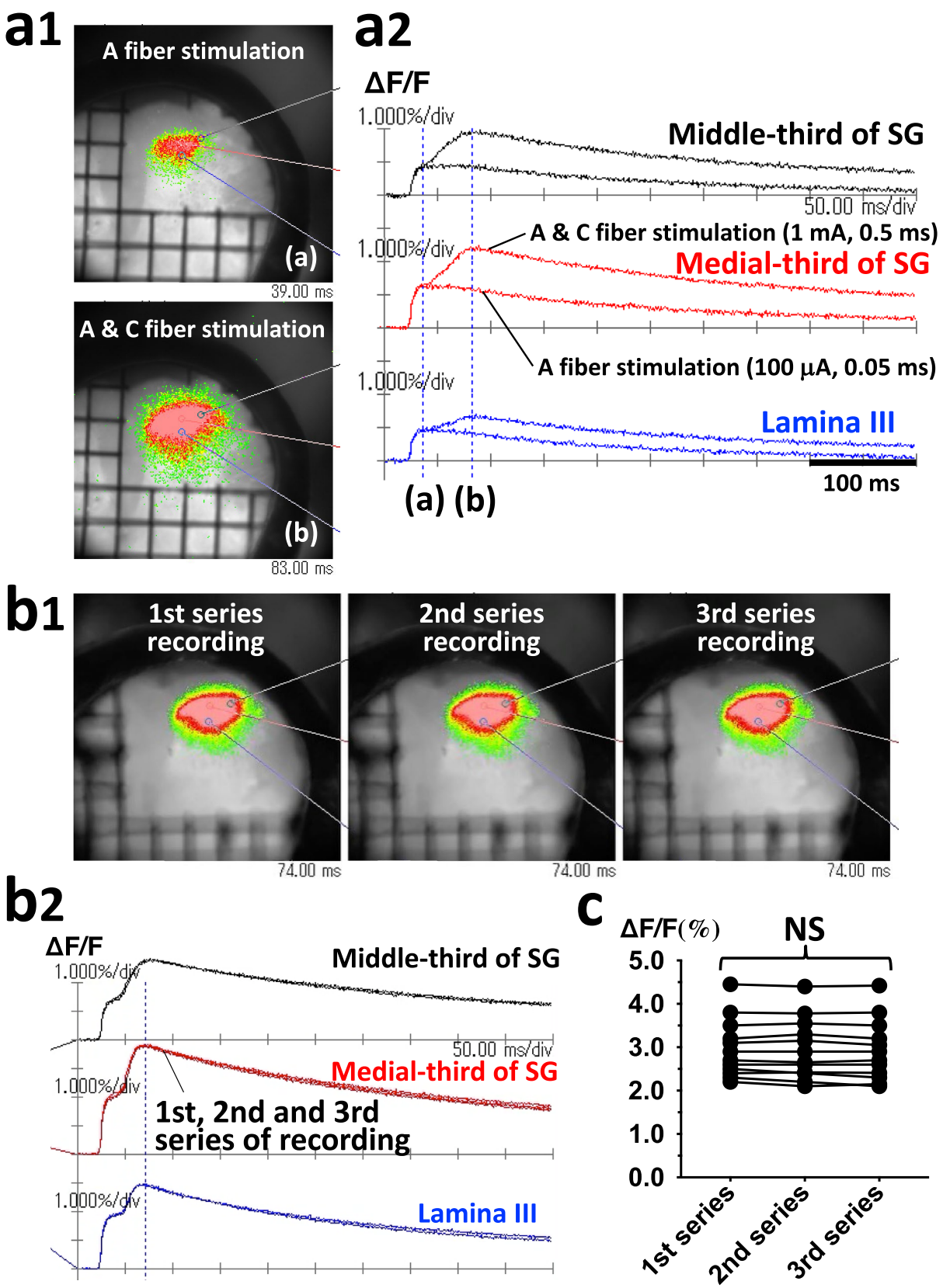
a1
A fiber stimulation
(a)
39.00 ms
A & C fiber stimulation
(b)
83.00 ms
a2
ΔF/F
1.000%/div
Middle-third of SG
50.00 ms/div
A & C fiber stimulation (1 mA, 0.5 ms)
Medial-third of SG
A fiber stimulation (100 μA, 0.05 ms)
Lamina III
100 ms
(a) (b)
b1
1st series recording
2nd series recording
3rd series recording
74.00 ms
74.00 ms
74.00 ms
b2
ΔF/F
1.000%/div
Middle-third of SG
50.00 ms/div
Medial-third of SG
1st, 2nd and 3rd series of recording
Lamina III
c
ΔF/F(%)
NS
5.0
4.0
3.0
2.0
1.0
0.0
1st series
2nd series
3rd series

◂**Fig. 3** Dorsal root stimulation increases intracellular Ca^{2+} concentration. **a** In each series of recordings, changes in the fluorescence intensity relative to the initial intensity of fluorescence in each pixel (ΔF/F) were measured at three locations of the dorsal horn (medial-third and middle-third of SG and lamina III). The A-fiber intensity stimulation evoked a monophasic $[Ca^{2+}]_{in}$ response, whereas C-fiber intensity stimulation evoked a biphasic response. Images (a) and (b) in **a1** were obtained at time points indicated by dotted blue lines (a) and (b) in **a2**. **b** Images of three repeated recordings at 10-min intervals. $[Ca^{2+}]_{in}$ responses were evoked by C-fiber intensity stimulation. Each image in **b1** was obtained at the peak time point indicated by the dotted blue line in **b2**. The fluorescence intensity changes (ΔF/F) of the first, second, and third series of recordings shown in **b1** are superimposed (**b2**). **c** No change in the peak of fluorescence intensity changes (ΔF/F) indicated by the dotted blue line in **b2** was observed by repeated stimuli and recordings. Data were analyzed using repeated measures one-way ANOVA (NS; not significant, $p = 0.1101$, $n = 12$)

Staining spinal cord slice with Ca^{2+} indicator

Slices prepared for optical recording were stained with the Ca^{2+} indicator, Rhod-2 AM (0.01% Rhod-2 AM in ACSF). After Rhod-2 AM (0.33 mg) was dissolved in oxygenated ACSF (3.3 mL), this staining solution was further bubbled with a gas mixture (95% O_2 and 5% CO_2) in a 10-mL syringe (Fig. 2a) for 15 min at slightly below room temperature (15–20 °C). Owing to its hydrophobic nature, Rhod-2 AM was insoluble in water, and thus adequate stirring and sonication were necessary to dissolve it in ACSF, which resulted in the release of dissolved gases (O_2, CO_2) from the dye solution. To ensure viability of the spinal cord during staining, further oxygenation of the staining solution was required. The slices were then immersed in the staining solution (Fig. 2b) within a staining chamber (Fig. 2c) for 120–150 min; the staining solution was continuously bubbled with a gas mixture (95% O_2 and 5% CO_2; 20–25 mL/min). The staining chamber was placed in a sealed container; the mixed gas was pumped into the container to maintain the internal pressure at 50–80 cmH_2O (Fig. 2d). This setup allows PCO_2, PO_2, pH, and temperature of the staining solution to be maintained at 40–50 mmHg, over 700 mmHg, 7.3–7.4, and 18–20 °C, respectively, for several hours during staining (Fig. 2e).

Intracellular Ca^{2+}-imaging and dorsal root stimulations

A single Rhod-2-loaded slice was placed in a measuring chamber (volume: 0.6 mL) on the fluorescence microscope stage and superfused with ACSF (15–20 mL/min) equilibrated with 95% O_2 and 5% CO_2. The slice was allowed to stabilize for at least 30 min. The ACSF temperature was maintained at 36–37 °C throughout the recording. Drugs were introduced by replacing the initial ACSF with another ACSF containing a known drug concentration without altering the perfusion rate or temperature. The perfusion system was identical to that used in our previous electrophysiological experiments.

An optical recording system (MiCAM03-N256; Brain Vision Co., Tokyo, Japan) was used for recording and analysis. Each slice was exposed to an excitation wavelength of 530 nm (510–550 nm) from an LED lamp (LEX-3G; Brain Vision Co.) and observed with a low-magnification objective lens (PLAN APO; Olympus, Tokyo, Japan). The emission wavelengths that passed through the optical filter (> 580 nm) were captured using a tandem-type fluorescence microscope (THT Macroscope; Brain Vision Co.). Fluorescence images were recorded using a high-speed CMOS camera (MiCAM03-N256; Brain Vision Co.), and data analysis was performed using MiCAM03 software (BV Ana; Brain Vision Co.). Each image comprised 256 × 256 pixels, with a field of view of 2.64 × 2.64 mm.

The L5 dorsal root was stimulated with a single pulse using a suction electrode (Fig. 1d) to induce depolarizing activity in the dorsal horn. Stimulation intensities were 100 μA (0.05 ms) for A-fibers and 1000 μA (0.5 ms) for both A- and C-fibers. Thresholds for stimulation intensity and duration for Aa/β, Aδ and C-fibers with this suction electrode have been established previously [10].

Fluorescence intensity changes relative to the initial intensity of fluorescence in each pixel (ΔF/F) were recorded at 1 frame/1.0 ms, usually for 500 ms. In some experiments, signals were recorded for 2.0 s to measure the duration of fluorescence changes. In each Ca^{2+} imaging series, stimulation and recording were repeated 15 times at 20-s intervals, and the signals were averaged to produce a series of $[Ca^{2+}]_{in}$ images. The ratio of the fractional change in Rhod-2 fluorescence intensity in each pixel to the pre-stimulation intensity (ΔF/F) was calculated and used as the optical signal. The increase in $[Ca^{2+}]_{in}$ was defined as ΔF/F. Optical signals were obtained from almost all areas of the dorsal horn (Supplemental Video 1). However, in this study, signals from three representative locations of the dorsal horn (medial-third and middle-third of the substantia gelatinosa (SG) and lamina III) were analyzed separately [7]. The ΔF/F peaks were selected from the most intense response area, typically located in the SG's medial-third [7]. These peak ΔF/F values were used to evaluate the effects of drugs.

Whole-cell patch-clamp recording from SG neurons

In some experiments, whole-cell patch-clamp recordings were performed after Ca^{2+} imaging using the same slices. Under a dissecting microscope with transmitted illumination, the SG was identifiable as a relatively densely stained band across the superficial dorsal horn (Fig. 1C). However, the contours of individual SG neurons were not visible, necessitating blind gigaohm sealing. Patch pipettes were

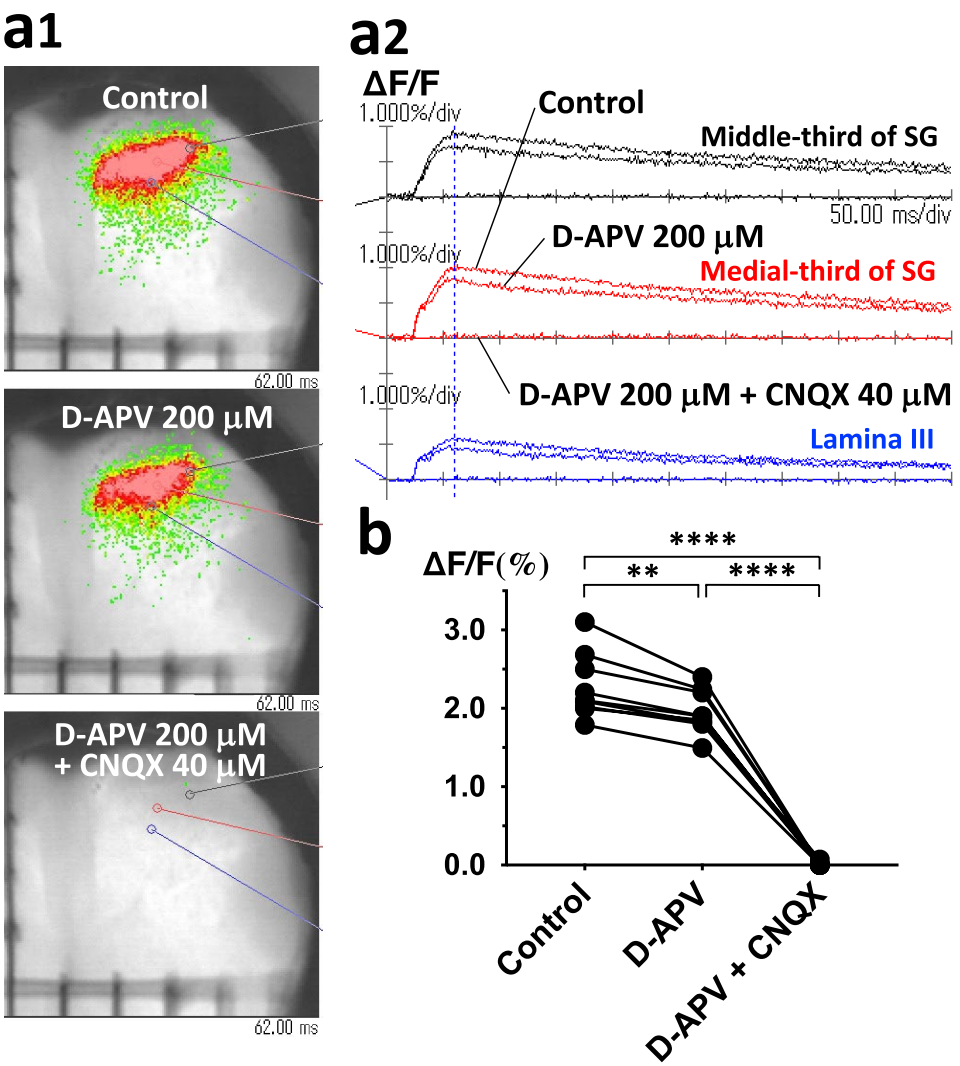

Fig. 4 Blockade of glutamate receptors abolishes dorsal root stimulation-evoked intracellular Ca^{2+} responses. **a** The maximum $[Ca^{2+}]_{in}$ response was partially suppressed by D-APV (200 μM) while almost eliminated by simultaneous administration of APV (200 μM) and CNQX (40 μM). Each image in **a1** was obtained at the time point indicated by the blue dotted line in **a2**. **b** The effects of D-APV and CNQX on the maximum $[Ca^{2+}]_{in}$ response were analyzed by repeated measures one-way ANOVA followed by Bonferroni's multiple comparisons test (**p = 0.0012, ****p < 0.0001, n = 9). D-APV, D-2-amino-5-phosphonovaleric acid; CNQX, 6-cyano-7-nitroquinoxaline-2,3-dione

fabricated from thin-walled borosilicate glass capillary tubing (1.5 mm o.d.; World Precision Instruments, Sarasota, FL, USA), with typical resistances of 5–10 MΩ when filled with the internal solution (in mM): K-gluconate 135, KCl 5, $CaCl_2$ 0.5, $MgCl_2$ 2, EGTA 5, HEPES 5, and ATP-Mg salt 5.

After establishing the whole-cell configuration, voltage-clamped neurons were held at -70 mV to record excitatory postsynaptic currents (EPSCs). Excitatory postsynaptic potentials (EPSPs) and action potentials were recorded under current-clamp conditions. The L5 dorsal root was stimulated using the same suction electrode used in the $[Ca^{2+}]_{in}$ imaging study. Monosynaptic EPSCs were identified based on their constant latency with graded intensity and high-frequency repetitive stimulation (20 Hz) [10]. Membrane currents and potentials were amplified using an Axopatch 200B amplifier (Molecular Devices, Union City, CA, USA). Data were stored on a personal computer using pCLAMP 10.7 software (Molecular Devices).

Drugs

Drugs were sourced as follows: Rhod-2 AM from AnaSpec (Fremont, CA, USA); dimethyl sulfoxide (DMSO), 6-cyano-7-nitroquinoxaline-2,3-dione (CNQX), and bicuculline from Wako Pure Chemical Industries (Osaka, Japan); remimazolam besilate from Mundipharma (Tokyo, Japan); bupivacaine hydrochloride from Sigma-Aldrich (St. Louis, MO, USA); morphine hydrochloride from Shionogi Pharma (Osaka, Japan); D-2-amino-5-phosphonovaleric acid (D-APV) from Cayman Chemical (Ann Arbor, MI, USA); and tranexamic acid (TXA) from LKT Laboratories (St. Paul, MN, USA). All drugs were prepared as stock solutions in distilled water or DMSO and were diluted to the required concentrations in ACSF immediately before bath perfusion. Rhod-2 AM was dissolved in DMSO and stored at – 20 °C. Immediately before staining, Rhod-2 AM was diluted to approximately 0.01% in ACSF (0.33 mg/3.3 mL).

Statistical analyses

Data are presented as means ± standard deviations (SDs). Statistical analyses were performed using repeated measures one-way analysis of variance (ANOVA), followed by Bonferroni's post hoc multiple comparisons tests for the $[Ca^{2+}]_{in}$ imaging data. Statistical significance was set at $P < 0.05$. GraphPad Prism 9 (GraphPad, San Diego, CA, USA) was used for statistical analysis.

Results

Ca^{2+} signals in the spinal dorsal horn in response to dorsal root stimulation

Intracellular Ca^{2+} fluorescent signals were used to visualize the intensity and spread of neural excitation in the dorsal horn. Single electrical stimulation of the dorsal root at A-fiber intensity elicited a monophasic change in optical signals, while simulation at C-fiber intensity produced a biphasic change, mainly in the superficial dorsal horn, including lamina II (SG, Fig. 3a). The initial phase of the response was attributed to input from primary afferent A-fibers, while the subsequent phase (after a delay of 20–30 ms) was due to the input from both A- and C-fibers. The most intense signals were consistently observed in the medial-third of the SG in both A- and C-fiber intensity stimulations, making this location suitable for evaluating the effects of repeated stimuli and drugs on the intensity of neural excitation [7].

We assessed the impact of photobleaching due to repeated stimulation and recording on $[Ca^{2+}]_{in}$ imaging. Figure 3b1 and b2 display the first, second, and third series of recordings with a 10-min interval. Contrary to findings by Hirahara et al. [6] and in our previous method [7], no significant changes in peak signal intensity were observed across these three repeated stimuli (Fig. 3c, NS: not significant, $P = 0.1101$, $n = 12$). These results indicated that photobleaching effects due to repeated measurements were negligible. Therefore, regarding experiments lasting less than approximately 1 h, the raw data of dorsal root stimulation-induced fluorescence changes obtained in the initial imaging series (without drug application) could serve as a control for fluorescence changes in subsequent imaging series (with drug application).

Ca^{2+} signals are derived from postsynaptic dorsal horn neuron activity rather than from presynaptic axon terminals

The recorded $[Ca^{2+}]_{in}$ response is thought to be primarily mediated by postsynaptic voltage-gated Ca^{2+} channels and N-Methyl-d-aspartate (NMDA) receptor channels in dorsal horn neurons. However, some involvement of voltage-gated Ca^{2+} channels in presynaptic axon terminals cannot be excluded. We investigated the extent to which $[Ca^{2+}]_{in}$ at presynaptic axonal terminals is involved in the recorded $[Ca^{2+}]_{in}$ responses by completely blocking postsynaptic glutamate receptors.

Figure 4 shows that bath application of D-APV (200 µM), an NMDA receptor antagonist, reduced the C-fiber intensity stimulation-induced $[Ca^{2+}]_{in}$ response to 86.5 ± 4.5% of the control value (**$P = 0.0012$, $n = 9$). Co-application of D-APV (200 µM) and CNQX (40 µM), an α-amino-3-hydroxy-5-methyl-4-isoxazolepropionic acid (AMPA) receptor antagonist, nearly abolished the dorsal root-evoked $[Ca^{2+}]_{in}$ response (Fig. 4b, 0.4 ± 1.1% of the control value, ****$P < 0.0001$, $n = 9$). These findings indicated that the recorded $[Ca^{2+}]_{in}$ responses were derived from the postsynaptic soma and dendrites of dorsal horn neurons rather than from the presynaptic axon terminals of primary afferents and/or interneurons in the dorsal horn.

Relationship between Ca^{2+} signals and electrophysiological responses

We examined the temporal and spatial resolutions of this method. Figure 5a shows the initial rise in primary afferent-evoked $[Ca^{2+}]_{in}$ responses in the medial-third of the SG. An elevated $[Ca^{2+}]_{in}$ response was detected in the medial-third of the SG 4 ms after dorsal root stimulation (Fig. 5b), which became stronger and more widespread with each millisecond. In dorsal horn neurons, initial action potential generation occurs 2–3 ms after dorsal root (~ 25 mm) stimulation. Therefore, $[Ca^{2+}]_{in}$ is expected to rise almost simultaneously with the first action potential. Thus, this method provides millisecond-level resolution for visualizing the rise and spatial spread of the $[Ca^{2+}]_{in}$ response during the rising phase.

In some experiments ($n = 10$), whole-cell patch-clamp recordings of SG neurons were performed using the same slice after the $[Ca^{2+}]_{in}$ imaging study. Figure 6 illustrates that the rising phases of the A-fiber-and C-fiber-evoked $[Ca^{2+}]_{in}$ responses aligned exactly with the onset of A-fiber-and C-fiber-evoked monosynaptic EPSCs, respectively (Fig. 6a, b). However, the falling phase of the $[Ca^{2+}]_{in}$ response differed from the persistence of action potential generation. Action potential generation was mostly limited to the rising phase of $[Ca^{2+}]_{in}$ elevation, while $[Ca^{2+}]_{in}$ remained elevated even when the membrane potential returned to the resting membrane potential (Fig. 6c, d). In SG neurons stimulated by C-fiber intensity, action potentials never persisted beyond 120 ms ($n = 24$ from 10 slices; Fig. 6d), whereas the elevated $[Ca^{2+}]_{in}$ response lasted approximately 2.0 s, with a half-decay time of 401.7 ± 21.5 ms ($n = 19$; Fig. 6c).

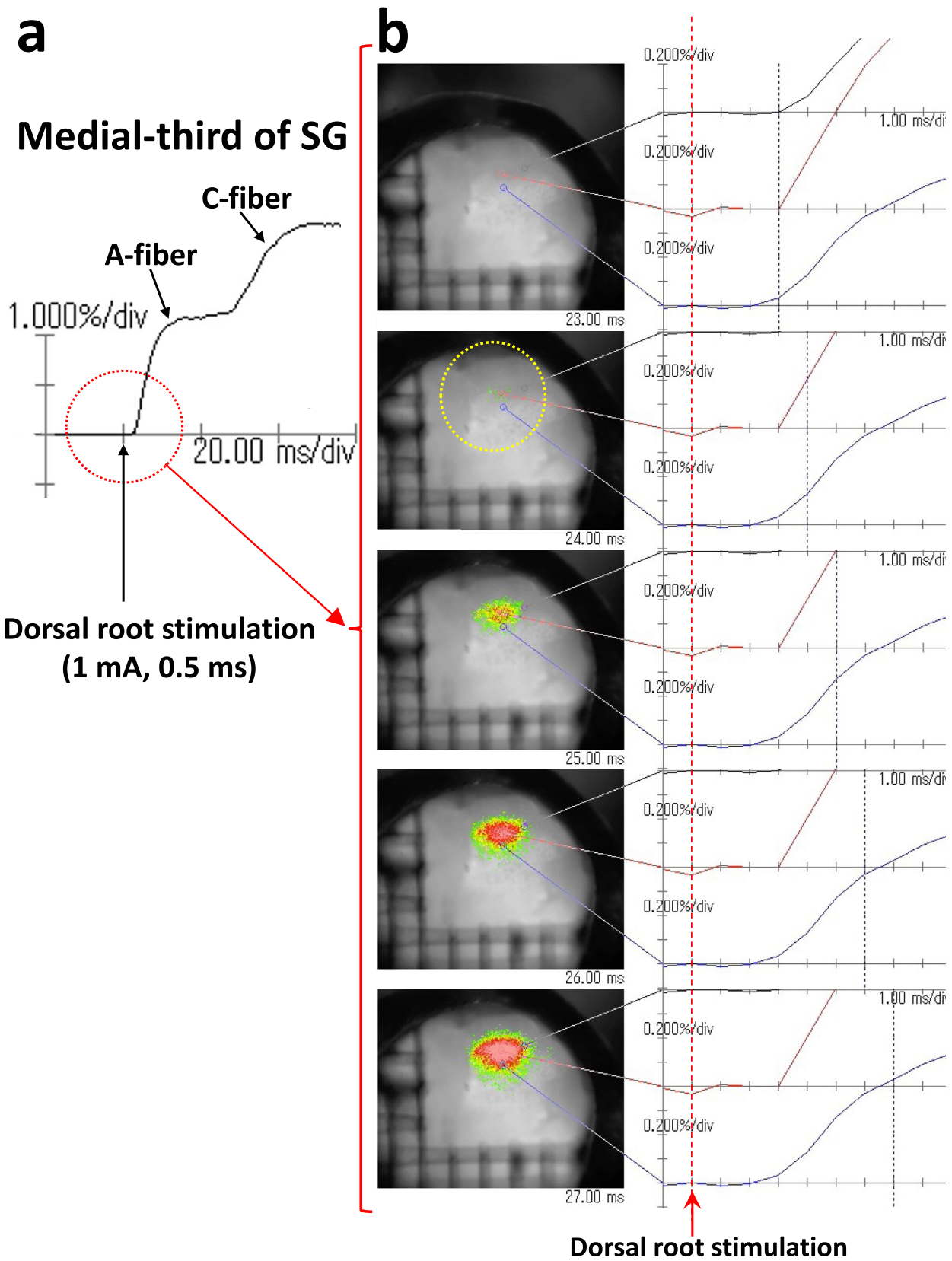
a
Medial-third of SG
C-fiber
A-fiber
1.000%/div
20.00 ms/div
Dorsal root stimulation
(1 mA, 0.5 ms)
b
0.200%/div
1.00 ms/div
23.00 ms
24.00 ms
25.00 ms
26.00 ms
27.00 ms
Dorsal root stimulation

◂**Fig. 5** Temporal and spatial resolution of intracellular Ca^{2+} imaging. **a** The rising phases of the A- and C-fiber-evoked $[Ca^{2+}]_{in}$ responses. The red dotted circle indicates the first rising point of A-fiber-evoked $[Ca^{2+}]_{in}$ response. **b** The red dotted circle in **a** is shown enlarged at 1-ms intervals. Note that the image of the first $[Ca^{2+}]_{in}$ response is detected in the medial third of SG (within the yellow dotted circle) 4 ms after dorsal root stimulation. SG, substantia gelatinosa

Thus, the elevated $[Ca^{2+}]_{in}$ response in the falling phase does not correspond to action potential generation, indicating that the rising phase (particularly the peak value of the Ca^{2+} fluorescent signal) is essential for evaluating neural excitation.

Effects of analgesics, anesthetics, and hyperalgesics on Ca^{2+} signals

Using these characteristics, we investigated the effects of morphine, a typical opioid analgesic, on dorsal root stimulation-induced $[Ca^{2+}]_{in}$ responses. Figure 7 shows that morphine inhibited the dorsal root stimulation-induced $[Ca^{2+}]_{in}$ response in a concentration-dependent manner, with C-fiber-evoked components being highly sensitive to morphine at low nanomolar concentrations (Fig. 7a1, a2). Maximum morphine inhibitory effect was observed at approximately 1–10 μM (Fig. 7b1, b2).

Additionally, we evaluated the effects of bupivacaine, a local anesthetic. Morphine (10 μM) significantly reduced the peak value of the dorsal root C-fiber intensity stimulation-evoked $[Ca^{2+}]_{in}$ response (43.9 ± 4.9% of control value, ****P < 0.0001, n = 8), while bupivacaine (0.5 mM) completely abolished the $[Ca^{2+}]_{in}$ response (0% of control value; Fig. 8a, b, Supplementary Video 2).

Next, we assessed the effects of remimazolam, a short-acting intravenous benzodiazepine anesthetic. Remimazolam (10 μM) did not significantly alter dorsal root stimulation-evoked $[Ca^{2+}]_{in}$ responses (98.0 ± 2.0% of control value, P = 0.0656, n = 8). However, subsequent morphine administration significantly inhibited the response (44.8 ± 4.4% of the control value, ****P < 0.0001, n = 8; Fig. 9, Supplemental Video 3).

Finally, we evaluated the effects of bicuculline and TXA. Bicuculline, a γ-aminobutyric acid $(GABA)_A$ receptor antagonist, induces allodynia and hyperalgesia in animals when administered into the spinal subarachnoid space [11]. TXA may exert hyperalgesic effects in both animals and humans [12, 13]. Bicuculline (40 μM) significantly increased the intensity of dorsal horn neuron excitation in response to A-fiber stimulation (288.4 ± 48.4% of control value, ****P < 0.0001, n = 10; Fig. 10). The duration and spatial spread of excitation were also significantly increased (Fig. 10a1, a2, Supplemental Video 4). These effects were almost completely blocked by D-APV (200 μM), an NMDA receptor antagonist (106.8 ± 8.6% of the control value, NS; not significant, P = 0.0776; Fig. 10b). Conversely, TXA (1 mM) did not significantly alter dorsal root stimulation-evoked $[Ca^{2+}]_{in}$ responses (113.0 ± 10.8% of control value, P = 0.0780, n = 8), but higher TXA concentrations (3, 10 mM) significantly increased the intensity, duration, and spatial spread of excitation (132.6 ± 19.9%, 152.6 ± 25.3%, **P = 0.0095 and **P = 0.0032, respectively, n = 8; Fig. 11a, b). However, bicuculline (40 μM) was more potent than the high-concentration TXA (10 mM; Fig. 11ae, Supplemental Video 5).

Discussion

Intracellular Ca^{2+} concentration increases rapidly with action potential onset, providing evidence that an action potential has occurred in the cell. The rapid increase in intracellular Ca^{2+} concentration can be measured optically by placing a Ca^{2+} indicator that has the property of increasing fluorescence intensity into the cell at a certain wavelength as the intracellular Ca^{2+} concentration increases. However, almost all researchers in this field use young animals, approximately 1–2 weeks old. The low myelin content of the central nervous tissue of juvenile animals allows the Ca^{2+} indicator to enter target neurons relatively easily, even with short staining times. In addition, spinal cord tissue from juvenile animals is resistant to hypoxia during staining (20–30 min). Conversely, spinal cord tissue from mature animals is myelin-rich and sensitive to hypoxia. Therefore, in the spinal cord of juvenile animals, Ca^{2+} indicator could reach the spinal cord cells without much concern about the partial pressure of oxygen or temperature in the staining solution. However, we, anesthesiologists, are interested in nociceptive signaling in the normal mature spinal cord and in pathological spinal cord (e.g., after peripheral nerve injury), not in fetal or neonatal neurotransmission.

The most significant improvement in our method is its ability to supply sufficient oxygen and a Ca^{2+} indicator to neuronal cells in the slice during staining (over 2–3 h) without continuous perfusion. The amount of dissolved oxygen in the dye solution was maintained by increasing the external pressure during dyeing so that the oxygen partial pressure in the dye solution was sufficiently maintained even with a small amount of mixed gas bubbling. In addition, precise control of the staining solution temperature reduced oxygen consumption of the spinal cord cells without causing aggregation of the Ca^{2+} indicator. These improvements allowed for adequate time for the dye to penetrate the slices, facilitating clear, rapid, and nearly photobleach-free intracellular Ca^{2+} imaging of fully mature adult rat spinal cord slices with long dorsal roots, which is technically challenging.

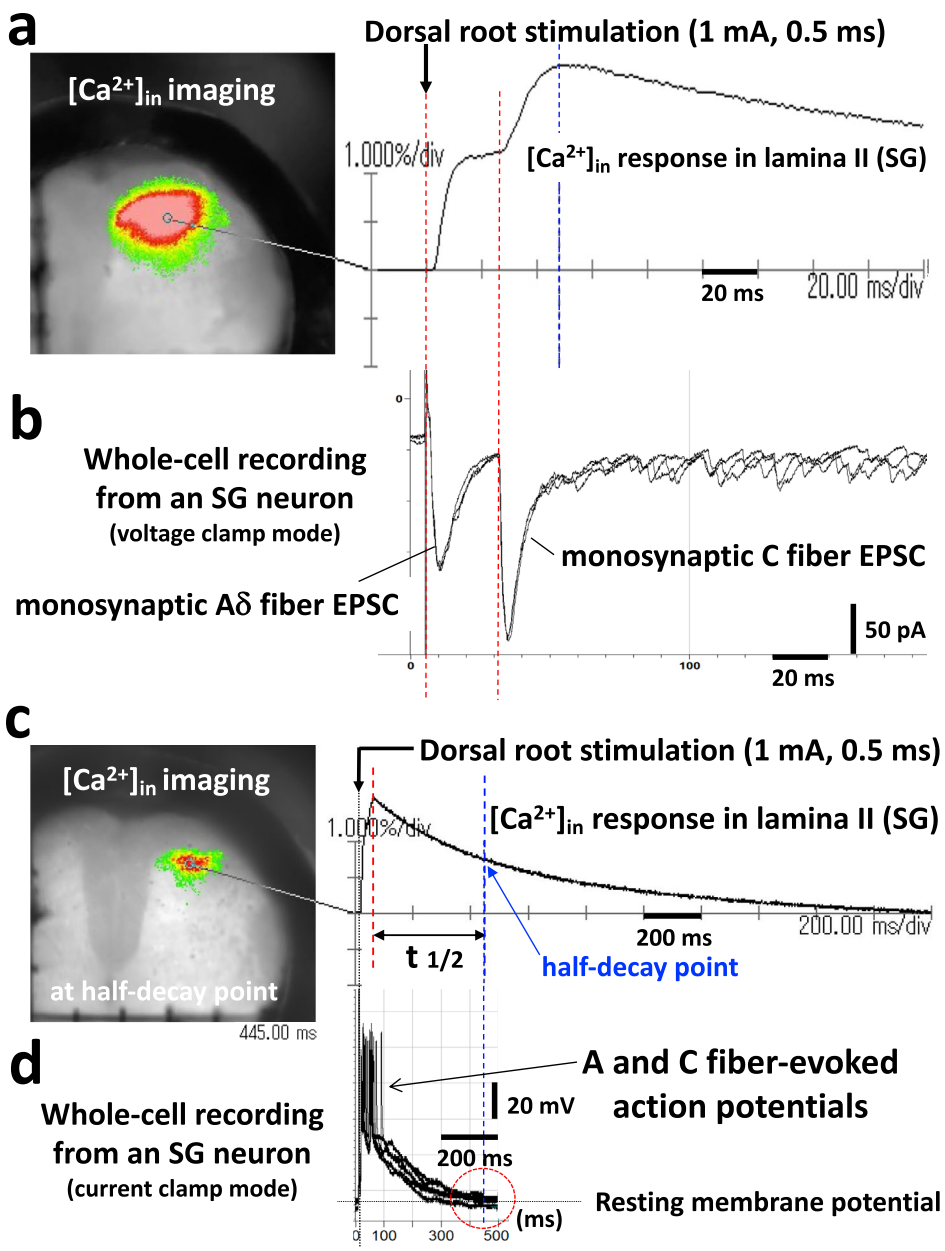

Fig. 6 Relationship between intracellular Ca^{2+} elevation response, excitatory postsynaptic current, and action potential generation. **a** A-and C fiber-evoked $[Ca^{2+}]_{in}$ elevation. The A-fiber-evoked component was followed by a C-fiber component. The image (**left**) shows the maximum point of $[Ca^{2+}]_{in}$ response, as indicated by the blue dotted line (**right**). **b** Whole-cell recording from an SG neuron, voltage clamped to -70 mV. The dorsal root was stimulated to evoke A- and C-fiber-mediated fast monosynaptic EPSCs (**b, right**). $[Ca^{2+}]_{in}$ imaging (**a**) and whole-cell recording (**b**) were obtained from the same slice, and their traces were recorded on the same timescale. The onset of $[Ca^{2+}]_{in}$ elevation by A- and C-fibers coincided with the onset of monosynaptic A- and C-fiber-evoked EPSCs, respectively. **c** Dorsal root stimulation-evoked $[Ca^{2+}]_{in}$ elevation lasting approximately 2 s. The maximum $[Ca^{2+}]_{in}$ response is indicated by the red dotted line (**right**). The image on the **left** corresponds to the time point of half decay of the $[Ca^{2+}]_{in}$ response, indicated by the blue dotted line (**right**). The half-decay times ($t_{1/2}$) were 395.0 ms in this slice. **d** Whole-cell recording in current-clamp mode from an SG neuron. A- and C-fiber-evoked EPSPs and their action potentials were recorded. The duration of action potential generation was mostly limited to the rising phase of $[Ca^{2+}]_{in}$ elevation, whereas $[Ca^{2+}]_{in}$ elevation persisted even when the membrane potential returned to the resting membrane potential level. At the half-decay point indicated by the blue dotted line (**c**, **right**), the membrane potential had already returned to the resting level, and no action potential was generated (**d,** red dotted circle). The data for **c** and **d** were obtained from the same slice, and their traces were on the same timescale. EPSCs, excitatory postsynaptic currents; EPSPs, excitatory postsynaptic potentials; SG, substantia gelatinosa

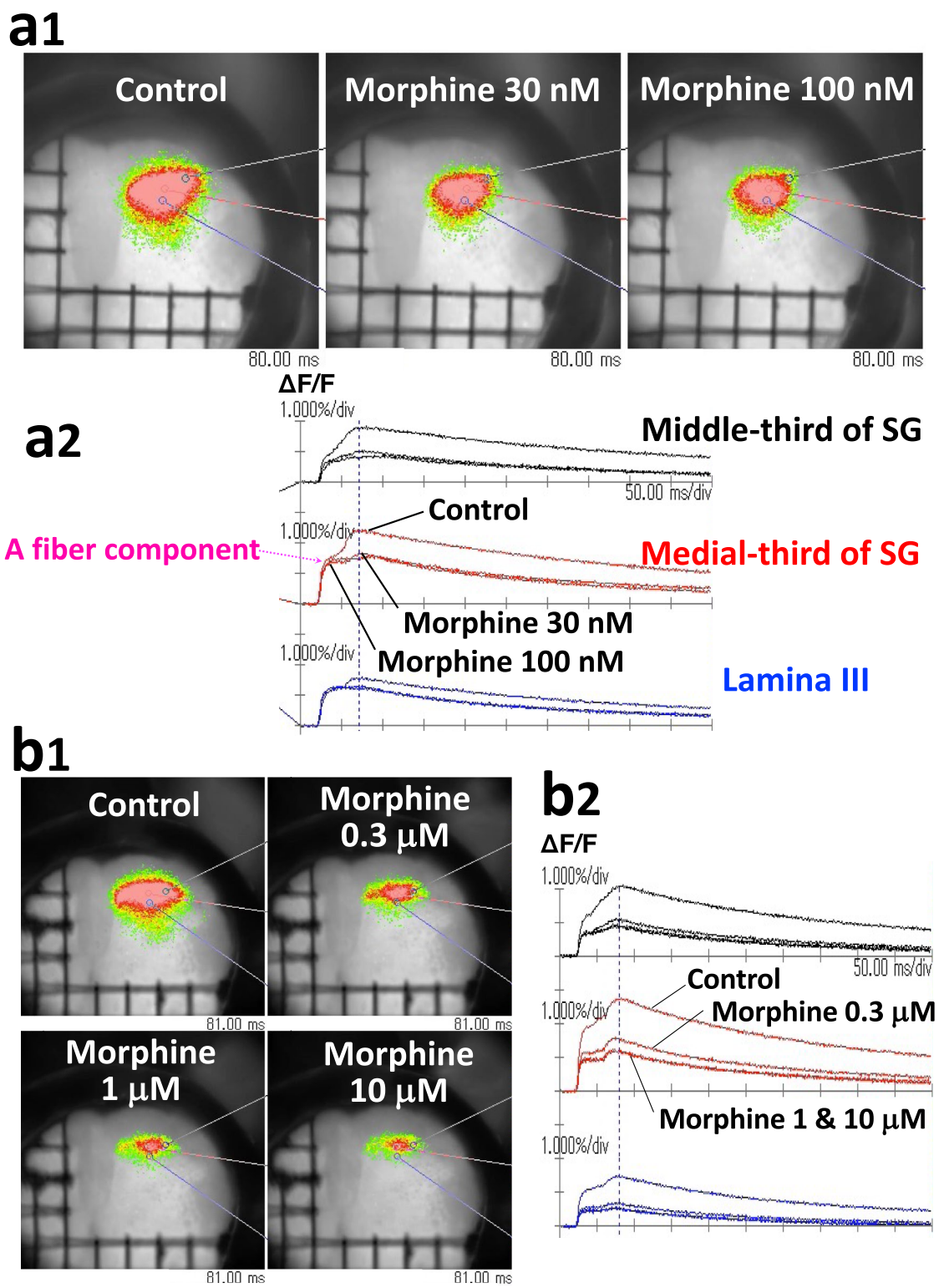

Fig. 7 Morphine inhibits the intracellular Ca^{2+}-elevation response elicited by dorsal root stimulation. **a** Each image in **a1** was obtained at the time point indicated by the blue dotted line in **a2**. C-fiber-evoked components were highly sensitive to morphine at concentrations as low as the nanomolar range (30 nM, 100 nM), while the A-fiber-evoked component was almost unaffected. **b** The inhibitory effect of morphine reached a maximum in the 1—10 micromolar concentration range. Each image in **b1** was obtained at the time point indicated by the blue dotted line in **b2**

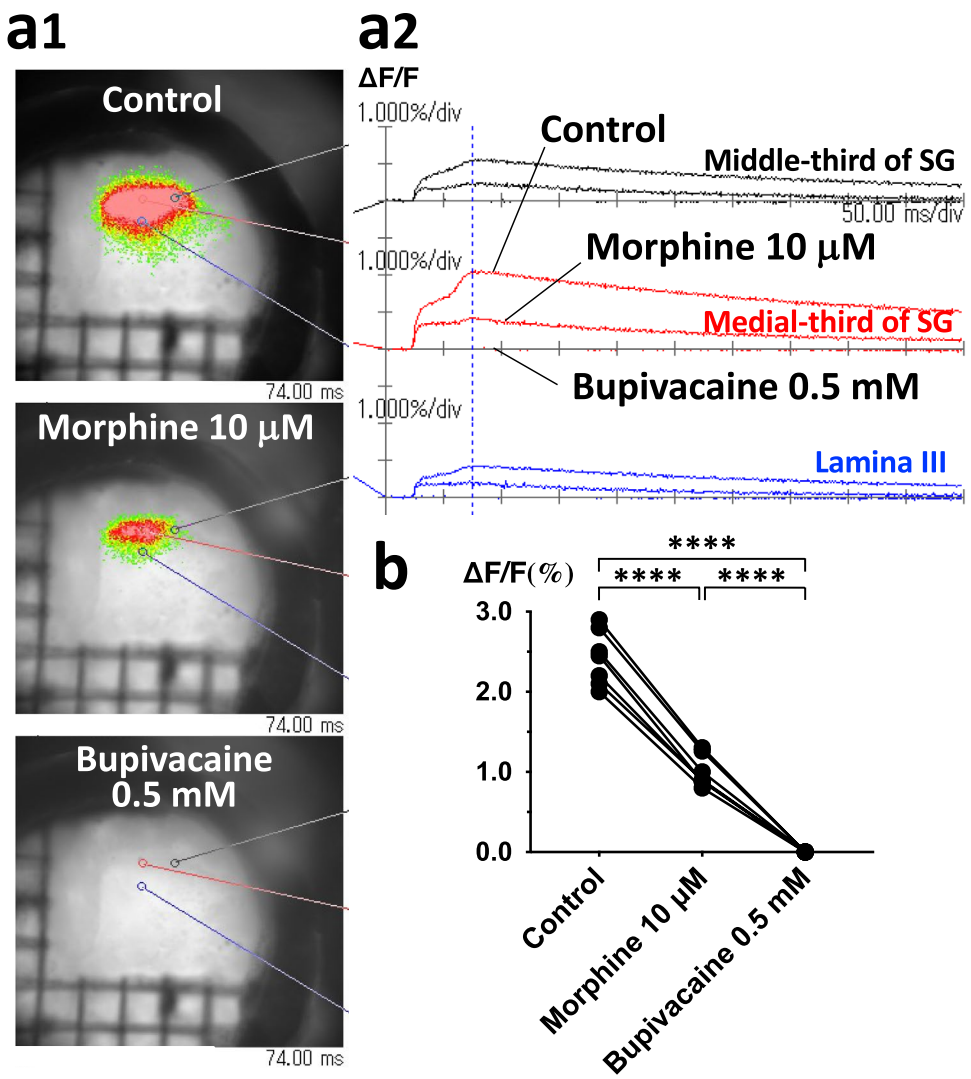

Fig. 8 Differences in action between morphine and bupivacaine on intracellular Ca^{2+} response. **a** Morphine inhibits the $[Ca^{2+}]_{in}$ response, but even concentrations as high as 10 μM do not eliminate it. In contrast, bupivacaine (0.5 mM) completely abolished it. Each image in **a1** was obtained at the time point indicated by the blue dotted line in **a2**. **b** Morphine (10 μM) significantly decreased the $[Ca.^{2+}]_{in}$ responses, which were eliminated by 0.5 mM bupivacaine (****$p < 0.0001$, $n = 8$, repeated measures one-way ANOVA followed by Bonferroni's multiple comparisons test)

Intracellular Ca^{2+} imaging

Nociceptive signaling in the dorsal horn of the spinal cord has been studied primarily using electrophysiological techniques, such as intracellular [8, 9] and whole-cell patch-clamp recordings [10, 14]. Although electrophysiological experiments remain the gold standard for studying neuronal activity, they have some limitations. They can record from only one cell at a time, making determining the spatial and temporal extent of neuronal activity impossible. Furthermore, these methods are complex and time-consuming. Conversely, our method enables visualization of the intensity, spatial distribution, and temporal dynamics of spinal neuronal excitations, thereby addressing the disadvantages of whole-cell patch-clamp recordings of single cells.

Voltage-sensitive dyes are commonly used to detect membrane potential changes in targeted cells and identify excited neurons optically [15]. However, intracellular Ca^{2+} concentration changes follow sodium ion influx into cells, which causes neuronal membrane depolarization [16]. Thus, intracellular Ca^{2+} measurement can also be used to visualize excited neurons, albeit somewhat indirectly [1, 2]. Optical properties, such as changes in absorbance and fluorescence intensity, are more pronounced with intracellular Ca^{2+} indicators than voltage-sensitive dyes [4]. Since both voltage-sensitive dyes and Ca^{2+} indicators struggle to penetrate myelin-rich tissues such as the spinal cord, Ca^{2+} indicators are more advantageous for visualizing spinal dorsal horn neuron excitation. Additionally, the $[Ca^{2+}]_{in}$ elevation response observed in this study was entirely abolished by the co-application of NMDA and AMPA receptor antagonists, indicating that this method does not detect $[Ca^{2+}]_{in}$ elevation in presynaptic axonal terminals. Since neuronal axons lack voltage-gated Ca^{2+} channels except at their terminals, this characteristic makes Ca^{2+} imaging methods more advantageous than do membrane potential imaging methods when assessing dorsal horn cell activity as it excludes $[Ca^{2+}]_{in}$ changes in axonal terminals.

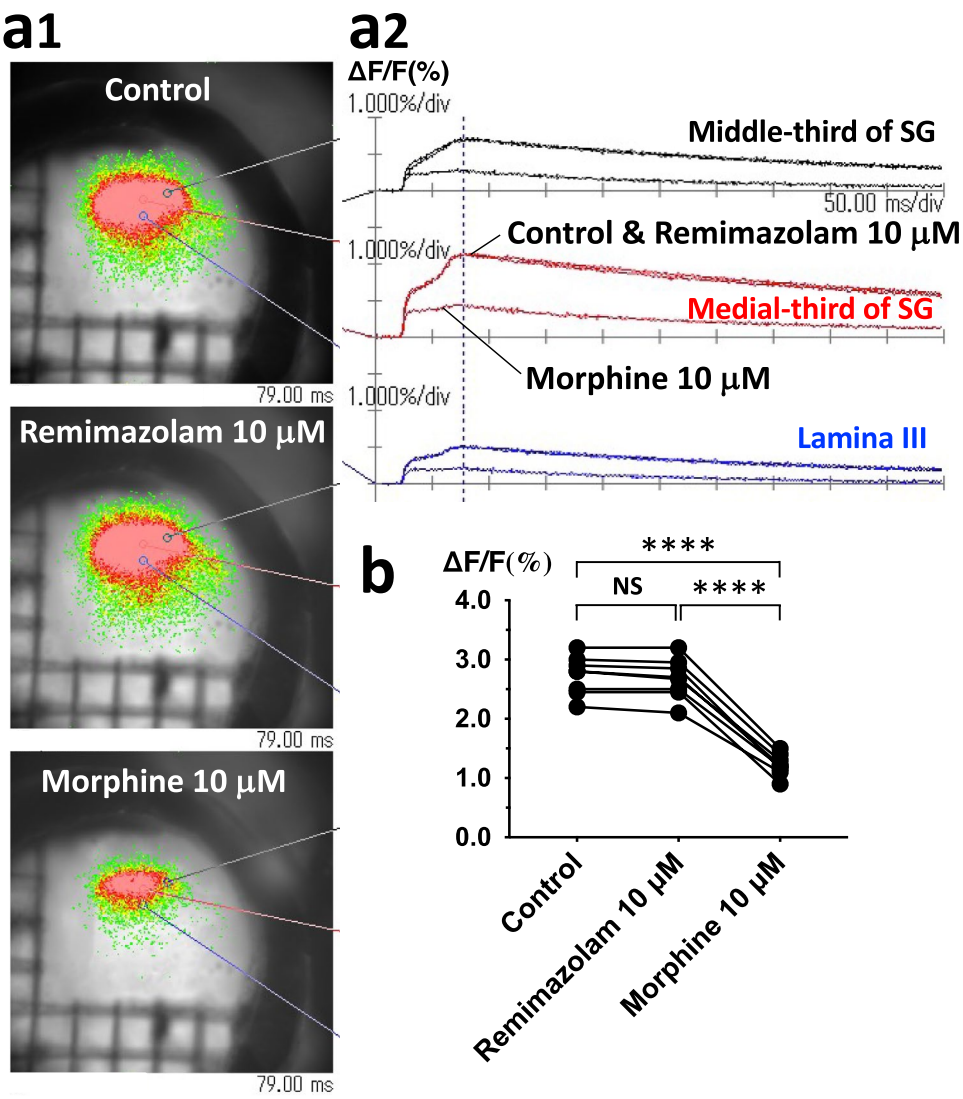

Fig. 9 Remimazolam has little effect on intracellular Ca^{2+} responses. **a** Remimazolam applied at 10 μM did not affect the $[Ca^{2+}]_{in}$ response, which was significantly suppressed by subsequently administering morphine (10 μM). Each image in **a1** was obtained at the time point indicated by the blue dotted line in **a2**. **b** Remimazolam (10 μM) did not significantly affect the $[Ca^{2+}]_{in}$ response (NS; not significant, $p = 0.0656$, $n = 8$). In contrast, morphine (10 μM) significantly decreased the $[Ca^{2+}]_{in}$ response (****$p < 0.0001$, $n = 8$, repeated measures one-way ANOVA followed by Bonferroni's multiple comparisons test)

Dorsal root stimulation-evoked $[Ca^{2+}]_{in}$ responses in the dorsal horn

Dorsal root stimulation at intensities necessary to stimulate A-fibers elicited a monophasic response, whereas stronger stimuli that activate both A- and C-fibers produced a biphasic intracellular Ca^{2+} elevation response. These responses closely mirror the A- and C-fiber-evoked synaptic responses recorded previously using intracellular recordings and whole-cell patch-clamp techniques. Specifically, the latency of the two intracellular Ca^{2+} elevation responses corresponded precisely to the A- and C-fiber-evoked EPSCs (Fig. 6a). Furthermore, the timing of action potential onset coincided with the rising phase of $[Ca^{2+}]_{in}$. Therefore, the rising phase of $[Ca^{2+}]_{in}$ induced by dorsal root stimulation likely reflects the timing of action potential generation in dorsal horn cells and/or the expansion of their spatial excitation. Conversely, the falling phase of the $[Ca^{2+}]_{in}$ response was significantly slower than were the electrophysiological responses, with a half-decay time of approximately 400 ms. Even with sufficient dorsal root stimulation intensity to activate C-fibers, the generation of action potentials did not persist beyond 120 ms. Notably, the falling phase of $[Ca^{2+}]_{in}$ elevation represents the intracellular Ca^{2+} efflux process rather than neuronal excitation. Consequently, focusing on the rising phase, particularly the peak value, is more relevant when evaluating drug effects using this method.

Effect of analgesics, anesthetics, and hyperalgesics on the dorsal root-evoked $[Ca^{2+}]_{in}$ responses

Using the characteristics of the intracellular Ca^{2+} imaging method described, we first investigated the effects of morphine, a typical opioid analgesic. Morphine efficiently suppressed C-fiber-mediated responses at lower concentrations, suggesting that C-fiber-mediated pain was responsive

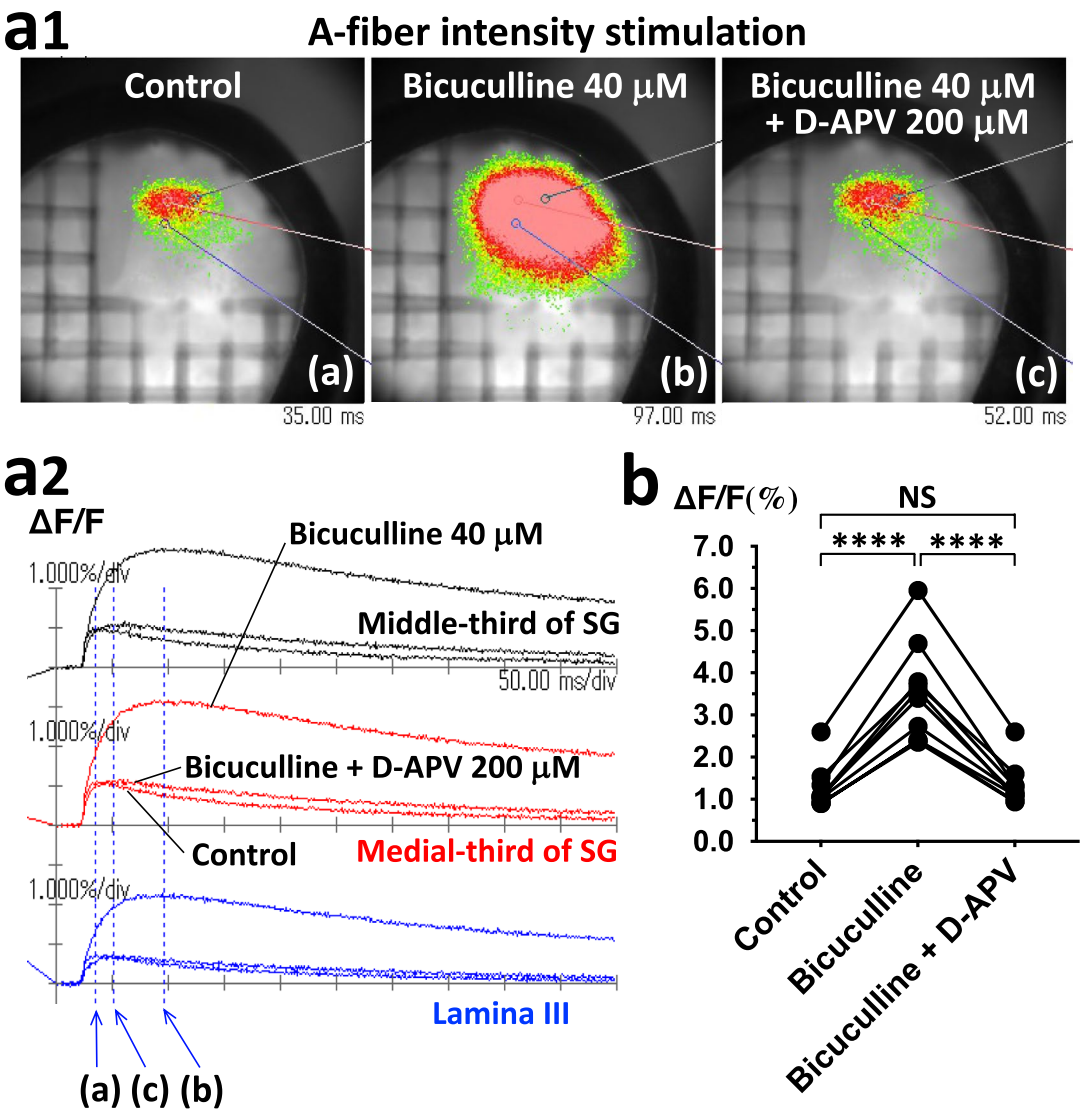

Fig. 10 Bicuculline potentiates intracellular Ca^{2+} responses. **a** Bicuculline (40 μM) enhanced the intensity, spatial extent, and duration of A-fiber evoked $[Ca^{2+}]_{in}$ responses, which were almost entirely reversed by D-APV. Each image **a** (35 ms), **b** (97 ms), **c** (52 ms) in **a1** was obtained at the time point indicated by the blue dotted line in **a2 a, b, c**. Note that the rising phase was prolonged by bicuculline. **b** Bicuculline significantly increased the peak of $[Ca^{2+}]_{in}$ responses (****$p < 0.0001$, $n = 10$), which were reversed by D-APV (NS; not significant compared to control, $p = 0.0776$, $n = 10$, repeated measures one-way ANOVA followed by Bonferroni's multiple comparisons test). D-APV, D-2-amino-5-phosphonovaleric acid

to opioid analgesics. At higher concentrations (micromolar range), the A-fiber component was suppressed, reaching its maximum effect at approximately 1–10 μM. Opioids more effectively suppress C-fiber-mediated pain, such as pain at rest, rather than pain occurring during body movement. Clinical concentrations of morphine in human cerebrospinal fluid (CSF) typically range between several micromoles and tens of micromoles when administered epidurally or subarachnoidally [17, 18]. Our results align well with those of clinical studies and experiences. Conversely, the local anesthetic bupivacaine eliminated the $[Ca^{2+}]_{in}$ response to dorsal root stimulation, reflecting its clinical equivalence to spinal anesthesia. We examined the effects of remimazolam, a short-acting benzodiazepine recently used as an intravenous anesthetic. Although benzodiazepines potentiate $GABA_A$ receptor activity and may exert analgesic effects on the spinal dorsal horn, remimazolam at 10 μM did not show a significant inhibitory effect, suggesting minimal clinical analgesic impact at this concentration. Benzodiazepines generally lack analgesic properties, a finding consistent with our clinical observations of remimazolam.

Finally, we evaluated the effects of hyperalgesic agents. Bicuculline induces allodynia and hyperalgesia when administered to the spinal cord [11]. Electrophysiological

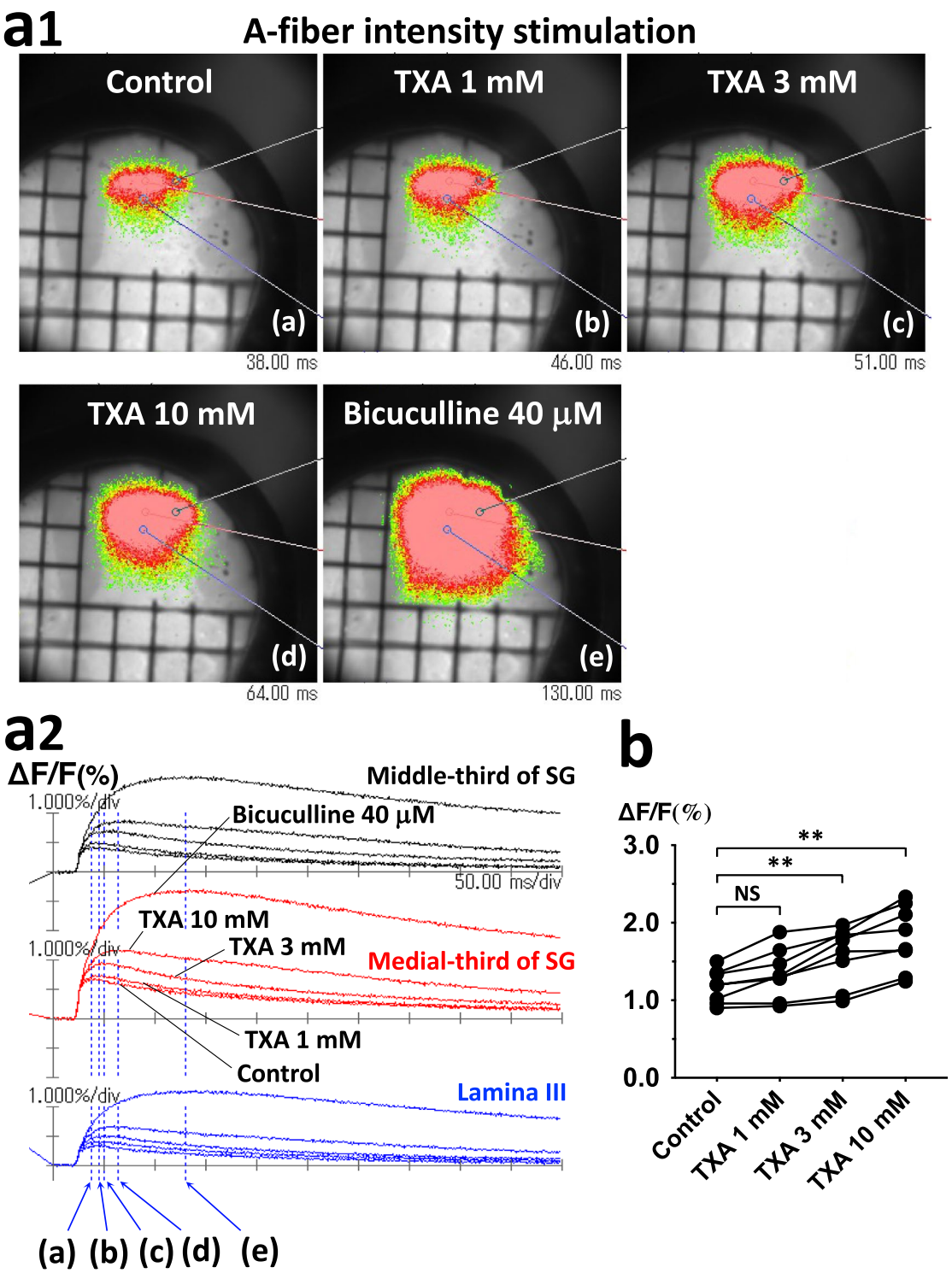

Fig. 11 High concentrations of tranexamic acid enhance intracellular Ca^{2+} responses. **a** TXA enhanced the intensity, spatial extent, and duration of $[Ca^{2+}]_{in}$ responses in a concentration-dependent manner. Each image (**a**–**e**) in **a1** was obtained at the time point indicated by the blue dotted line in **a2** (**a**–**e**, 38, 46, 51, 64, 130 ms, respectively). A high dose of TXA (3, 10 mM) enhanced the $[Ca^{2+}]_{in}$ responses, which was further augmented by bicuculline (40 μM, **a1**(**e**), **a2**). **b** TXA (3, 10 mM) significantly increased the peak of $[Ca^{2+}]_{in}$ responses (**p = 0.0095, **p = 0.0032 compared to control, respectively, n = 8), but the effect of TXA (1 mM) was not statistically significant (NS; not significant compared to control, p = 0.0780, n = 8, repeated measures one-way ANOVA followed by Bonferroni's multiple comparisons test). *TXA* tranexamic acid

studies have shown that bicuculline dramatically increases the response of dorsal horn neurons to dorsal root stimulation by blocking $GABA_A$ receptors [19, 20]. Our data demonstrated that bicuculline enhanced the intensity, duration, and spatial extent of A-fiber-evoked intracellular Ca^{2+} elevation responses, which the NMDA receptor antagonist, D-APV, almost entirely reversed, corroborating our previous electrophysiological studies [20]. TXA, which blocks $GABA_A$ and glycine receptors [13], exhibited unclear effects, unlike bicuculline, because of its dose-dependent nature, with significant effects only observed at very high concentrations. Ohashi et al. [12] have argued that intravenous administration of TXA has a hyperalgesic effect; however, our study found only weak effects, even at millimolar concentrations. Further information is required regarding the clinical CSF concentrations of TXA following intravenous administration.

Thus, this method is well-suited for screening drugs that potentially act at the spinal cord level and could be valuable in developing new analgesics. This method could also predict changes in spinal dorsal horn neuron excitability due to peripheral tissue nerve injury. An example is the hypothesis of intraspinal A fiber sprouting after peripheral nerve injury proposed by Woolf et al. [21]. Although this theory has now been debunked, there was much debate at the time. The most important focus of this hypothesis was whether A-fibers extending into the superficial layer would cause the lamina I, II neurons to become intensely excited. However, using our method, it could be easily demonstrated in a few experiments that the phenomenon of transmission of innocuous information to the nociceptive neurons in superficial layers of the dorsal horn via A-fiber does not occur (data not shown) after peripheral nerve injury.

Limitations

The method presented involves wide-area Ca^{2+} imaging, capturing the cumulative neural activity within a region rather than individual neural activities. For example, if increased neuronal activity is observed, wide-area Ca^{2+} imaging cannot distinguish whether it results from heightened activity within individual neurons or increased active neurons. Additionally, if a few neurons with different activity patterns are present among many neurons with synchronous activity, their activity may go undetected due to being obscured by many other neurons. If used appropriately, wide-area Ca^{2+} imaging can effectively capture the dynamics of macroscopic neural networks that are difficult to observe using other methods.

In conclusion, we developed a $[Ca^{2+}]_{in}$ imaging method using spinal cord slices with dorsal roots from fully mature adult rats and demonstrated that biphasic Ca^{2+} responses by A- and C-fibers can be recorded following dorsal root stimulation. Furthermore, the spatial spread of excitation to the surrounding neurons was also observed. These advantages address some limitations of whole-cell patch-clamp recordings of single dorsal horn neurons. This method is simple, convenient, and effective in studying nociceptive transmission in the dorsal horn of the spinal cord.

Supplementary Information The online version contains supplementary material available at https://doi.org/10.1007/s00540-024-03451-0.

Acknowledgements We thank Dr. Naoshi Fuwara (Ph.D.) for technical advice and Editage (www.editage.com) for English language editing.

Funding This study was financially supported by a Grant-in-Aid for Scientific Research (B) from H. Baba (20H03775).

Declarations

Conflict of interest The authors declare no conflict of interest.

References

1. Smetters D, Majewska A, Yuste R. Detecting action potentials in neuronal populations with calcium imaging. Methods. 1999;18:215–21.
2. Ikegaya Y, Le Bon-Jego M, Yuste R. Large-scale imaging of cortical network activity with calcium indicators. Neurosci Res. 2005;52:132–8.
3. Grewe BF, Helmchen F. Optical probing of neuronal ensemble activity. Curr Opin Neurobiol. 2009;19:520–9.
4. Osanai M, Tanaka S, Takeno Y, Takimoto S, Yagi T. Spatiotemporal properties of the action potential propagation in the mouse visual cortical slice analyzed by calcium imaging. PLoS ONE. 2010;5: e13738.
5. Hartung JE, Gold MS. GCaMP as an indirect measure of electrical activity in rat trigeminal ganglion neurons. Cell Calcium. 2020;89: 102225.
6. Hirahara M, Fujiwara N, Seo K. Novel trigeminal slice preparation method for studying mechanisms of nociception transmission. J Neurosci Methods. 2017;286:6–15.
7. Baba H, Petrenko AB, Fujiwara N. Clinically relevant concentration of pregabalin has no acute inhibitory effect on excitation of dorsal horn neurons under normal or neuropathic pain conditions: An intracellular calcium-imaging study in spinal cord slices from adult rats. Brain Res. 2016;1648:445–58.
8. Yoshimura M, Jessell TM. Primary afferent-evoked synaptic responses and slow potential generation in rat substantia gelatinosa neurons in vitro. J Neurophysiol. 1989;62:96–108.
9. Baba H, Yoshimura M, Nishi S, Shimoji K. Synaptic responses of substantia gelatinosa neurones to dorsal column stimulation in rat spinal cord in vitro. J Physiol. 1994;478:87–99.
10. Baba H, Doubell TP, Woolf CJ. Peripheral inflammation facilitates abeta fiber-mediated synaptic input to the substantia gelatinosa of the adult rat spinal cord. J Neurosci. 1999;19:859–67.
11. Onaka M, Minami T, Nishihara I, Ito S. Involvement of glutamate receptors in strychnine- and bicuculline-induced allodynia in conscious mice. Anesthesiology. 1996;84:1215–22.
12. Ohashi N, Ohashi M, Endo N, Kohno T. Administration of tranexamic acid to patients undergoing surgery for adolescent

idiopathic scoliosis evokes pain and increases the infusion rate of remifentanil during the surgery. PLoS ONE. 2017;12: e0173622.
13. Ohashi N, Sasaki M, Ohashi M, Kamiya Y, Baba H, Kohno T. Tranexamic acid evokes pain by modulating neuronal excitability in the spinal dorsal horn. Sci Rep. 2015;5:13458.
14. Furue H, Narikawa K, Kumamoto E, Yoshimura M. Responsiveness of rat substantia gelatinosa neurones to mechanical but not thermal stimuli revealed by in vivo patch-clamp recording. J Physiol. 1999;521:529–35.
15. Grinvald A, Lieke EE, Frostig RD, Hildesheim R. Cortical point-spread function and long-range lateral interactions revealed by real-time optical imaging of macaque monkey primary visual cortex. J Neurosci. 1994;14:2545–68.
16. Catterall WA. Voltage-gated calcium channels. Cold Spring Harb Perspect Biol. 2011;3: a003947.
17. Bigler D, Christensen BC, Eriksen J, Jensen HN. Morphine, morphine-6-glucuronide and morphine-3-glucuronide concentrations in plasma and cerebrospinal fluid during long-term high-dose intrathecal morphine administration. Pain. 1990;41:15–8.
18. Samuelsson H, Hedner T, Venn R, Michalkiewicz A. CSF and plasma concentrations of morphine and morphine glucuronides in cancer patients receiving epidural morphine. Pain. 1993;52:179–85.
19. Yoshimura M, Nishi S. Primary afferent-evoked glycine- and GABA-mediated IPSPs in substantia gelatinosa neurones in the rat spinal cord in vitro. J Physiol. 1995;482:29–38.
20. Baba H, Ji RR, Kohno T, Moore KA, Ataka T, Wakai A, Okamoto M, Woolf CJ. Removal of GABAergic inhibition facilitates polysynaptic a fiber-mediated excitatory transmission to the superficial spinal dorsal horn. Mol Cell Neurosci. 2003;24:818–30.
21. Woolf CJ, Shortland P, Coggeshall RE. Peripheral nerve injury triggers central sprouting of myelinated afferents. Nature. 1992;355:75–8.